JOURNAL OF SOLID STATE CHEMISTRY 65, 301–308 (1986)

Synthesis, Crystal Growth, Structural Determination, and Optical Absorption Spectroscopy of the Magnetoplumbite Type Compound $LaNiAl_{11}O_{19}$

F. LAVILLE,* M. PERRIN,* A. M. LEJUS,* M. GASPERIN,† R. MONCORGE,‡ AND D. VIVIEN*

Chimie Appliquée de l'Etat Solide, UA 302, ENSCP 11 rue P. et M. Curie—75231 Paris Cedex 05, France; †Laboratoire de Minéralogie Crystallographie, UA 09, Université Paris VI, 4 Place Jussieu 75230 Paris Cedex 05, France; and ‡Laboratoire de Physico-Chimie des Matériaux Luminescents UA 442, Université de Lyon I, 43 bd du 11 Novembre 1918 69622 Villeurbanne, France

Received November 4, 1985; in revised form February 7, 1986

Single crystals of $LaNiAl_{11}O_{19}$ have been grown from the melt using either the Verneuil flame fusion process or floating zone method. The resolution of the crystal structure indicates that this compound is of the distorted magnetoplumbite type (hexagonal $P6_3/mmc$) and that Ni is sheared between tetrahedral and octahedral sites of the spinel blocks. This compound has also been prepared in powdered form by annealing coprecipitates of amorphous oxides at medium temperature. The thermal evolution of the coprecipitates leading to the magnetoplumbite phase has been studied simultaneously by X-ray diffraction and diffuse reflectance spectroscopy. All the main transitions of electronic spectra of the $LaNiAl_{11}O_{19}$ have been assigned. The existence of a certain amount of octahedral Ni in this material makes it a possible candidate as infrared tunable laser. This potential application will be discussed in a forthcoming paper.

I. Introduction

Lanthanide hexaaluminates with magnetoplumbite like structure are currently under investigation in our Laboratory. These compounds present interesting optical properties: in the powdered form, they have been proposed for highly efficient phosphors (*1*); in the single-crystalline form, they may be good substrates for L.P.E. growth of hexaferrite thin films (*2*) and present interesting lasing characteristics. In the latter case we have demonstrated that, according to its properties (*3*), the lanthanum–neodymium hexaaluminate (L.N.A.) is a good candidate to replace the yttrium–aluminum–Garnet (Y.A.G.: Nd) high power IR emitting laser (*4, 5*).

Among the $LnMAl_{11}O_{19}$ materials, two series of compounds have been studied extensively: $LnMgAl_{11}O_{19}$ with *Ln*: La, Ce, Pr, Nd, Sm, Eu, Gd (*6*) and $LaMAl_{11}O_{19}$ with *M* = Mn, Co, Fe (*7*). All these compounds have been prepared as single crystals from the melt (*6, 7*). The crystal structure of several of them ($LaMgAl_{11}O_{19}$ (*3*), $LaMnAl_{11}O_{19}$ and $LaCoAl_{11}O_{19}$ (*8*)) has also been determined. They all belong to the

0022-4596/86 $3.00

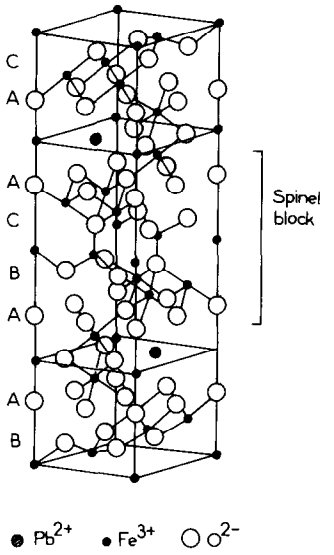

FIG. 1. Unit cell of the magnetoplumbite $PbFe_{12}O_{19}$.

magnetoplumbite ($PbFe_{12}O_{19}$) type structure. The unit cell is composed of spinel like blocks containing Al^{3+} and M^{2+} cations separated by mirror planes containing Al^{3+} and the Ln^{3+} cations (Fig. 1). In these compounds, the M^{2+} ions are of fundamental importance to ensure the thermodynamical stability of the structure. For example, it is not possible to grow from the melt single crystals of the magnetoplumbite type such as the lanthanum hexaaluminate $LaAl_{11}O_{18}$. However, crystal growth is readily accomplished with the addition of a small amount of M^{2+} ions (*9*). According to the structural investigations, the Co^{2+} and Mn^{2+} ions occupy only the (4f) (Wyckoff notation) of the $P6_3/mmc$ space group tetrahedral sites of the spinel blocks. This is also true for the Fe^{2+} ions on the basis of the absorption spectra of $LaFeAl_{11}O_{19}$ (*9*). These three transition metal ions are also known to preferentially occupy the tetrahedral sites of the spinel structure. In contrast, Ni^{2+} ions in $NiAl_2O_4$ lie mainly in octahedral coordination (*10*). This has prompted us to investigate the localization of the Ni^{2+} ions in the magnetoplumbite hexaaluminate $LaNiAl_{11}O_{19}$ in order to compare it with the previously studied isomorphs.

The magnetoplumbite compounds have also been proposed as host lattices for the immobilisation of radioactive wastes (*11*). For such an application, high temperature syntheses are inadequate, while methods such as coprecipitation in the amorphous state and annealing at low temperatures are more convenient. The present paper considers the elaboration of $LaNiAl_{11}O_{19}$ by such a method. The presence of Ni^{2+} ions in the spinel blocks of the structure allows us to follow the thermal behavior of the coprecipitate by optical absorption measurements. Our aim here is to extend the results of an earlier study with $EuMgAl_{11}O_{19}$ coprecipitates in which the optical probe ions Eu^{3+} are present in the mirror planes (*12*) instead of the spinel blocks.

II. Synthesis and Structural Determination of $LaNiAl_{11}O_{19}$ Single Crystals

(*a*) *Crystal Growth and Characterization*

Single crystals of $LaNiAl_{11}O_{19}$ have been obtained from the melt (≃1800°C) using either the Verneuil or the floating zone method. Details concerning apparatus and operating procedure have been given elsewhere (*7, 8*).

In the Verneuil process (flame fusion method), the starting powder is an intimate mixture of γ-Al_2O_3, La_2O_3, and NiO in appropriate proportions. The H_2/O_2 ratio of the oxyhydrogen torch which is usually equal to 3 has been lowered to 2.5 here in order to decrease the reducing power of the flame. This has been found necessary to avoid extensive loss of nickel during the crystal growth, NiO being partially reduced into metallic nickel when passing through the flame. The crystal growth starts on a sintered cone of the material and the rate of crystal growth is about 1 cm/hr. The blue

colored boules obtained are rod-shaped 20–30 mm length, 8–10 mm diameter. They consist of several large single crystals.

The starting rods used in the floating zone method are sintered mixtures of the same oxides. In this case, crystal growth starts on a single crystal seed and continues on by moving the molten zone along the rod at an approximate rate of 1 cm/hr. All the operations occur in air. The samples obtained are small cylinders, 20 mm in length and 5 mm in diameter. During cooling, thermal shock creates cracks in the sample which subsequently breaks into several single crystals of approximately $5 \times 5 \times 5$ mm^3 size.

In both methods, the growth occurs along the a crystallographic direction and there are always cleavage planes along (00.1). Powder X-ray diffraction patterns of ground crystals are characteristic of magnetoplumbite like compounds with $a = 5.57$ Å and $c = 22.01$ Å.

(b) Structural Determination

The structural investigations were performed on Verneuil single crystals. The X-ray diffraction intensities have been collected with a four-circle Philips PW 1100 X-ray diffractometer operating with the Mo$K\alpha$ radiation and using a $\theta/2\theta$ scanning at a rate of 0.025°/sec. Refinements of the structure have been obtained by taking into account 860 independant reflections. The starting parameters are those which have been previously determined for the parent compound $LaMnAl_{11}O_{19}$ (*8*).

It is immediately evident that the compound belongs to the magnetoplumbite type structure with the $AB_{12}O_{19}$ lattice, space group $P6_3/mmc$, and $Z = 2$. However, the Fourier and difference Fourier maps show a noticeable atomic shift compared to the ideal unit cell.

The main differences are the following:

—The Al_5 atom with theoretical position (2b) is split on two equivalent (4e) positions $(0.0.1/4 \pm \varepsilon)$. Hence, this atom has a tetrahedral environment instead of the fivefold coordination expected for its theorical position in the mirror plane.

—Besides lanthanum (La_1) in the normal position (2d) in the mirror plane, a small fraction of lanthanum occupies three statistically equivalent sites of a second type (La_2, (6h)), slightly shifted from the theorical one (0.667, 0.333, 0.25).

The adjustments of the atomic parameters have been achieved starting first with a statistical distribution of the Ni^{2+} ions over all the aluminum sites and using the average atomic diffusion factor

$$f = \frac{f(Ni^{2+}) + 11f(Al^{3+})}{12}.$$

After adjustment of the multiplicity factors and of the coordinates of the lanthanum ions it appears that, with respect to the electron densities of Al_3 and Al_4 sites which remain homogeneous, the size of the Al_5 site is smaller while those of the Al_1 and Al_2 sites are greater. It follows that the Al_5 site is completely free of Ni^{2+} ions while in the Al_1 and Al_2 sites, they are in excess compared to the statistical distribution. The final adjustments lead to a R factor of 5.3%. The residual electron density of the last difference Fourier map is very small, lower than $1e^-$ per Å^3.

The atomic parameters so obtained are gathered in Table I and the cation–oxygen distances are given in Table II. From these results it should be emphasized that in $LaNiAl_{11}O_{19}$, the Ni^{2+} ions are mainly distributed between the (2a) (Al_1) octahedra and the (4f) (Al_2) tetrahedra which both lie in the middle of the spinel blocks. It is not possible so far to make a quantitative estimate of the amount of Ni^{2+} ions in each type of site. However, if one considers the values of the temperature factors (Table I), the amount of Ni^{2+} ions in the tetrahedral sites appears greater than in the octahedral ones. One can notice that the mean

TABLE I

STRUCTURAL PARAMETERS OF THE REFINED STRUCTURE OF $LaNiAl_{11}O_{19}$

Atom	Wyckoff positions	Occupancy factor	× 10^4 x	y	z	B
La_1	2d	0.76	6667	3333	2500	0.4
La_2	6h	0.08	7199	4398	2500	0.7
Al_1	2a	1	0	0	0	0.5
Al_2	4f	1	3333	6667	274	0.2
Al_3	4f	1	3333	6667	1897	0.4
Al_4	12k	1	8318	6637	1078	0.4
Al_5	4e	0.5	0	0	2391	0.5
O_1	6h	1	1815	3631	2500	0.5
O_2	12k	1	1540	3081	523	0.35
O_3	12k	1	5043	86	1502	0.3
O_4	4e	1	0	0	1488	0.3
O_5	4f	1	6667	3333	562	0.3

"Al—O" distances (Al_1—O = 1.88 Å and Al_2—O = 1,82 Å) of the sites which are partly occupied by Ni ions are similar to the other Al—O distances and thus do not reflect the preference of the Ni^{2+} ions for these sites.

III. Investigation of the Synthesis of $LaNiAl_{11}O_{19}$ at Medium Temperature from Coprecipitates

(a) *Experimental Procedure*

Coprecipitation of amorphous La, Al, and Ni hydroxides is carried out by pouring the mixture, in appropriate proportions, of aqueous nitrate solutions of the corresponding metals into an excess of NH_4OH solution under vigourous stirring. After evaporation of the excess of liquid, the coprecipitate is dryed at 110°C and then calcined at 400°C in order to remove the ammonium nitrate. Then the coprecipitate is ground, compressed into pellets, and annealed for 20 hr at different temperatures.

Coprecipitation offers the advantage of achieving a phase pure product at moderate temperature (some 500°C less than by solid state reaction between oxides). Furthermore, it ensures that there no loss of reducible or volatile oxides and that the proper stoichiometry of the compound is retained.

The thermal behavior of the coprecipitate has been investigated as follows:

—by means of X-ray diffraction patterns in order to determine the nature of the phases which form and

—with the aid of diffuse reflectance spectroscopy to establish which kinds of sites the optically active Ni^{2+} ions occupy.

(b) *X-Ray Investigation of the Structural Evolution of Coprecipitates as a Function of Annealing Temperature*

The results are summarized in Table III. One observes that, starting from the amorphous state, the first stage of crystallization is the formation of a poorly crystallized f.c.c. oxygen sublattice as revealed by the appearance of broad (400) and (440) lines of the spinel lattice. It is well known in spinel compounds that these lines are mainly due to the oxygens. With increasing temperature, these two lines narrow while new lines characteristic of the spinel lattice begin to appear. This indicates that the Al and Ni ions are organizing themselves in their pre-

TABLE II

CATION ENVIRONMENTS IN $LaNiAl_{11}O_{19}$

La(1)	O(1) × 6	2,6940 Å
	O(3) × 6	2,7867
La(2)	O(1) × 2	2,3725
	O(1) × 2	2,8075
	O(3) × 2	2,5918
Al(1)	O(2) × 6	1,8792
Al(2)	O(2) × 3	1,8128
	O(5)	1,8402
Al(3)	O(3) × 3	1,8631
	O(1) × 3	1,9739
Al(4)	O(3) × 2	1,8339
	O(4)	1,8556
	O(5) × 3	1,9545
Al(5)	O(1) × 3	1,7666
	O(4)	1,9837
	O(4)	2,4617

TABLE III

X-RAY DIFFRACTION ANALYSIS OF PHASES FORMED BY ANNEALING OF COPRECIPITATES WITH NOMINAL COMPOSITION $LaNiAl_{11}O_{19}$ (W = WEAK, m = MEDIUM, S = STRONG)

T (°C)	Spinel $NiAl_2O_4$-γAl_2O_3	Perowskite $LaAlO_3$	Magneto-plumbite
350		Amorphous	
670		Amorphous	
800	Broadlines		
900	W	W	
1000	m	S	mW
1100	WW	mS	m
1200		m	mS
1300		mW	S
1400		W	SS

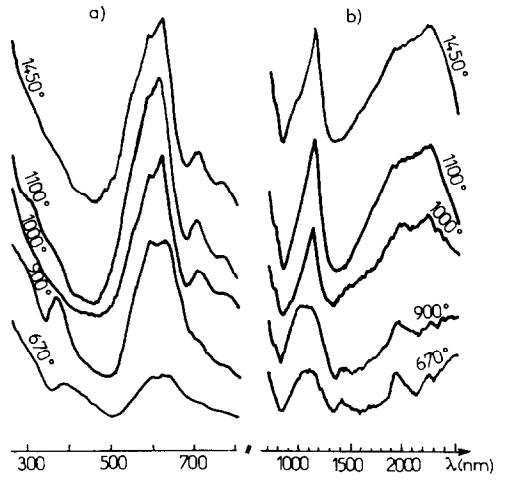

FIG. 2. Evolution with temperature of annealing of the diffuse reflectance spectra of amorphous coprecipitates with nominal composition $LaNiAl_{11}O_{19}$ (for the (b) series, the optical density scale has been expanded by a factor of 2).

ferred sites leading to a $NiAl_2O_4$–γ-Al_2O_3 solid solution. $LaAlO_3$ perowskite appears at 900°C. In contrast to the spinel phase, the perowskite is well crystallized as soon as it forms. The magnetoplumbite phase $LaNiAl_{11}O_{19}$ begins to appear at 1000°C. It forms at the expense of the spinel and perowskite phases and is almost complete by 1450°C. However, it is possible to obtained a pure magnetoplumbite phase at lower temperatures by increasing the duration of the annealing treatment. This behavior is similar to the previously reported thermal evolution of the coprecipitate with starting composition $EuMgAl_{11}O_{19}$ (*12*).

(c) *Evolution of the Diffuse Reflectance Spectra of Coprecipitates*

The diffuse reflectance spectra have been recorded at room temperature on a Beckman 5270 spectrometer fitted with an integration sphere. The reference powder was $BaSO_4$ and the spectral range 200–2400 nm.

A selection of the spectra for several annealing temperatures is given in Figs. 2a and b. At temperatures up to 900°C, there are no drastic changes in the spectra. These spectra coincide with those of a separate preparation of amorphous coprecipitates of the starting composition $NiAl_2O_4$ annealed at 900°C. The bands are characteristics of Ni^{2+} ions in a spinel phase in which they lie both in tetrahedral and octahedral sites according to the partially inverted character of the $NiAl_2O_4$ spinel phase (*10*). When the annealing temperature is increased, several modifications of the spectra, related to the formation of the magnetoplumbite hexaaluminate phase occur. In particular, bands or shoulders located around 370, 590, and 1080 nm weaken, while others around 625, 1130, and 2230 nm evolve (Figs. 3a and b).

The first series of lines is attributed to Ni^{2+} in octahedral symmetry, while the second one arises from nickel in tetrahedral environment. By 1100°C, the spectra do not change any more and this can be correlated with the disappearance of the spinel phase (Table III).

It should be noted that the formation of the magnetoplumbite lattice occurs via transfer of some octahedral nickel ions into

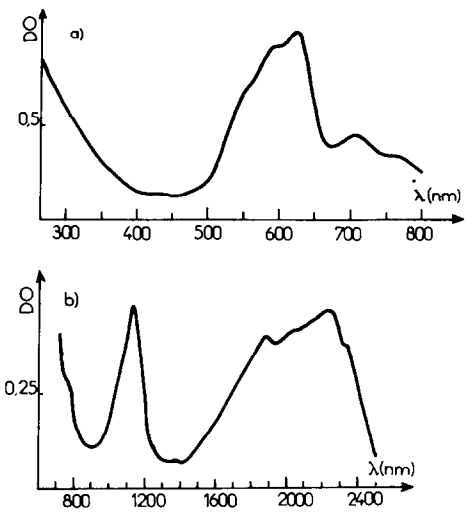

FIG. 3. Room temperature diffuse reflectance spectrum of a $LaNiAl_{11}O_{19}$ powder obtained by grinding of single crystals.

the tetrahedral sites. Hence, compared to the spinel case, the Ni^{2+} ions present a marked preference for a tetrahedral environment in agreement with the crystal structure determination (cf. Section II.b). This is particularly remarkable since the amount of tetrahedral sites in the magnetoplumbite lattice including the Al_5 positions is only 1/4 of the amount of the small cation sites instead of 1/3 in the spinel lattice.

IV. Assignment of the Optical Transitions in $LaNiAl_{11}O_{19}$

In order to attempt an identification of the different bands of the optical reflectance spectra of $LaNiAl_{11}O_{19}$, diffuse reflectance spectra of a $LaNiAl_{11}O_{19}$ powder prepared by grinding single crystals of this compound have been studied. The main features of these spectra (Fig. 3) are identical to those of the last terms of the coprecipitate series (Fig. 2), however, the resolution is somewhat better.

It has been already demonstrated that this compound contains both tetrahedral (T) and octahedral (O) Ni^{2+} sites. For each of these two site symmetries, one expects three spin allowed transitions between the spin triplet ground state ($^3A_2(^3F)$ in the case of octahedral symmetry, $^3T_1(^3F)$ in the case of tetrahedral symmetry) to the various excited states of same spin multiplicity. The energy of these transitions depends on the parameters Dq_O and Dq_T which measure the strength of the respective crystal fields and the electronic repulsion Racah parameters B_O and B_T. Using the formula given in the literature (*13*), the results concerning absorption spectra of Ni^{2+} in other matrices (*14, 15*) and the thermal evolution of the coprecipitates described in Section III.c, it is possible to associate these allowed transitions with the particular peaks or shoulders observed experimentally. The results are given in Table IV and Fig. 3. The spectral parameters used to fit these energies are $Dq_O = 1075\ cm^{-1}$ and $B_O = 780\ cm^{-1}$ for the octahedral symmetry and $Dq_T = 480\ cm^{-1}$ and $B_T = 845\ cm^{-1}$ for the tetrahedral symmetry. The ratio Dq_T/Dq_O is 0.45 which is very close to the theoretical value 4/9. These values must be considered as only approximative, and they could well differ from the real ones by as much as 10%. Indeed the overlapping of the tetrahedral and octahedral bands around 600 and 1100 nm can lead to some misattributions. This might be particularly true for the attribution of the octahedral nickel bands since the in-

TABLE IV

ASSIGNMENT OF THE ALLOWED OPTICAL TRANSITIONS OF Ni^{2+} OBSERVED IN THE DIFFUSE REFLECTANCE SPECTRUM OF $LaNiAl_{11}O_{19}$

Type of Ni^{2+} site	Transitions	λ observed (nm)	λ calculated (nm)
Octahedra (2a)	ν_{O_1}: $^3A_{2g} \rightarrow {}^3T_{1g}(^3P)$	370	365
	ν_{O_2}: $^3A_{2g} \rightarrow {}^3T_{1g}(^3F)$	590	589
	ν_{O_3}: $^3A_{2g} \rightarrow {}^3T_{2g}(^3F)$	1080	930
Tetrahedra (4f)	ν_{T_1}: $^3T_1 \rightarrow {}^3T_1(^3P)$	625	624
	ν_{T_2}: $^3T_1 \rightarrow {}^3A_2(^3F)$	1130	1127
	ν_{T_3}: $^3T_1 \rightarrow {}^3T_2(^3F)$	2230	2455

tensities of these bands are expected to be one order of magnitude weaker than the ones associated with the Ni^{2+} in the noncentrosymmetric tetrahedral sites—D_{3d} and C_{3v} site symmetry respectively. We also have neglected the influence of the spin-orbit coupling which could explain the splitting or shoulders observed for some bands. Moreover, most of the bands are phonon sidebands (electronic transitions accompanied by the simultaneous absorption or emission of lattice phonons); thus the energy of the associated electronic transitions that we need in the calculations should not be taken at the observed maxima, as we have done above, but at the position of the zero-phonon lines, when they are observable (generally, at low temperatures).

Finally spin forbidden transitions allowed via spin-orbit mixing may be responsible of some weaker bands observed in the spectra. For the value $Dq_T/B_T = 0.56$ one expects, according to the Tanabe-Sugano diagram for tetrahedral Ni^{2+} (*16*), four transitions from the $^3T_1$ ground state toward ^1E (^1G), $^1T_1(^1G)$ and $^1T_2(^1G)$ in the regions 400–500 nm and two others toward $^1T_2(^1D)$ and $^1E(^1D)$ around 750 nm. We do observe the latter transitions in our spectra around 710 and 770 nm, in agreement with what is found in $ZnO:Ni^{2+}$ (*17*). Tentative identification of the former is made difficult by the overlapping adjacent bands, although some shoulders occur in the experimental spectrum in the expected spectra range. Similarly, from the Tanabe-Sugano diagrams for octahedral Ni^{2+} and knowing that $Dq_O/B_O = 1.38$, two forbidden transitions are expected from the ground state toward $^1A_{1g}(^1G)$ and $^1T_{2g}(^1D)$ at about 450 nm and toward $^1E_g(^1D)$ at about 700 nm. Once again tentative assignments are difficult to make. More accurate attributions will be provided later in a forthcoming paper which is particularly devoted to the excitation and emission properties of $LaMgAl_{11}O_{19}(Ni^{2+})$ (*19*).

V. Conclusion

Lanthanum nickel hexaaluminate $LaNiAl_{11}O_{19}$ has been prepared either in the crystalline form from the melt or in powdered form by annealing of amorphous coprecipitates. In contrast to other $LaMAl_{11}O_{19}$ compounds (M = Co, Mn . . .) in which the divalent cations lie exclusively in the tetrahedral sites of the spinel blocks (as in the corresponding MAl_2O_4 spinels), in $LaNiAl_{11}O_{19}$, the Ni^{2+} ions are shared between the (4f) tetrahedral and (2a) octahedral sites. Such a mixed distribution also occurs in the $NiAl_2O_4$ spinel. However, the amount of Ni^{2+} ions in the tetrahedral sites is more important in the magnetoplumbite compound than in the spinel, showing that the attraction of the (4f) tetrahedral sites of the spinel blocks for divalent cations is rather strong in the magnetoplumbite lattice.

Because of the presence of octahedral Ni^{2+} in $LaNiAl_{11}O_{19}$ and the possibility of growing large single crystals of this compound or of the mixed one $LaNi_xMg_{1-x}Al_{11}O_{19}$, and also because another material of the same family has been shown valuable as a solid state laser (*4, 5*), these nickel activated materials are considered to be potential candidates for tunable infrared lasers (*18, 19*).

References

1. M. Tamatani, *Jpn. J. Appl. Phys.* **13,** 950 (1974); J. M. P. J. Verstegen, J. L. Sommerdijk, and J. G. Verriet, *J. Lumin.* **6,** 425 (1973); A. L. N. Stevels, *J. Lumin.* **20,** 99 (1979).
2. F. Haberey, R. Leckebusch, M. Rosenberg, and K. Sahl, *Naturwissenschaften* **68,** 376 (1981).
3. A. Kahn, A. M. Lejus, M. Madsac, J. Thery, D. Vivien, and J. C. Bernier, *J. Appl. Phys.* **52,** 6864 (1981).
4. D. Vivien, A. M. Lejus, J. Thery, R. Collongues, J. J. Aubert, R. Moncorge, and F. Auzel., *C.R. Acad. Sci. Paris II* **298,** 195 (1984).
5. L. D. Schearer, M. Leduc, D. Vivien, A. M. Lejus, and J. Thery, *IEEE J. Quantum Electr.* **22,** 713 (1986).

6. D. SABER AND A. M. LEJUS, *Mater. Res. Bull.* **16,** 1325 (1981).
7. F. LAVILLE AND A. M. LEJUS, *J. Cryst. Growth* **63,** 426 (1983).
8. M. GASPERIN, M. C. SAINE, A. KAHN, F. LAVILLE, AND A. M. LEJUS, *J. Solid State Chem.* **54,** 61 (1984).
9. F. LAVILLE, "Thèse de doctorat es-sciences physiques"—Paris (Université Pierre et Marie Curie), 1985.
10. P. PORTA, F. S. STONE, AND R. G. TURNER, *J. Solid State Chem.* **11,** 135 (1974).
11. J. THERY, D. VIVIEN, A. M. LEJUS, AND R. COLLONGUES, *Ann. Chim. Fr.* **10,** 397 (1985); P. E. D. MORGAN, D. R. CLARKE, C. M. JANTZEN, AND A. B. HARKER, *J. Amer. Ceram. Soc.* **64,** 249 (1981).
12. P. THUERY, F. LAVILLE, E. TRONC, A. M. LEJUS, AND D. VIVIEN, *Rev. Chim. Min.* **22,** 216 (1985).
13. K. F. PURCELL AND J. C. KOTZ, "Inorganic Chemistry," p. 567, Saunders, Philadelphia (1977); A. B. P. LEVER, "Inorganic Electronic Spectroscopy," 2nd ed., p. 126, Elsevier, Amsterdam (1984).
14. M. I. TEJEDOR-TEJEDOR, M. A. ANDERSON, AND A. J. HERBILLON, *J. Solid State Chem.* **50,** 153 (1983).
15. J. R. AKRIDGE AND J. H. KENNEDY, *J. Solid State Chem.* **29,** 63 (1979).
16. R. S. DRAGO, "Physical Methods in Chemistry," p. 643, Saunders, Philadelphia (1977).
17. R. PAPPALARDO, D. L. WOOD, AND R. C. LINARES, JR., *J. Chem. Phys.* **35**(4), 1460 (1961).
18. F. AUZEL AND R. MONCORGE, *J. Optics (Paris)* **15**(5), 338 (1984).
19. R. MONCORGE, T. BENYATTOU, D. VIVIEN, AND A. M. LEJUS, *J. Luminescence* **33,** 199 (1986).